



Title	Self-doping effect and successive magnetic transitions in superconducting Sr₂VFeAsO₃
Author(s)	Cao, GH; Ma, Z; Wang, C; Sun, Y; Bao, J; Jiang, S; Luo, Y; Feng, C; Zhou, Y; Xie, Z; Hu, F; Wei, S; Nowik, I; Felner, I; Zhang, L; Xu, Z; Zhang, FC
Citation	Physical Review B - Condensed Matter And Materials Physics, 2010, v. 82 n. 10
Issued Date	2010
URL	http://hdl.handle.net/10722/142470
Rights	Physical Review B (Condensed Matter and Materials Physics). Copyright © American Physical Society.

Self-doping effect and successive magnetic transitions in superconducting $\text{Sr}_2\text{VFeAsO}_3$ Guang-Han Cao,^{1,2,*} Zhifeng Ma,¹ Cao Wang,¹ Yunlei Sun,¹ Jinke Bao,¹ Shuai Jiang,¹ Yongkang Luo,¹ Chunmu Feng,¹ Yi Zhou,¹ Zhi Xie,³ Fengchun Hu,³ Shiqiang Wei,³ I. Nowik,⁴ I. Felner,⁴ Lei Zhang,⁵ Zhu'an Xu,^{1,2} and Fu-Chun Zhang^{1,6}¹*Department of Physics, Zhejiang University, Hangzhou 310027, China*²*State Key Laboratory of Silicon Materials, Zhejiang University, Hangzhou 310027, China*³*National Synchrotron Radiation Laboratory, University of Science and Technology of China, Hefei 230029, China*⁴*Racah Institute of Physics, The Hebrew University, Jerusalem 91904, Israel*⁵*High Magnetic Field Laboratory, Chinese Academy of Sciences, Hefei 230031, China*⁶*Department of Physics, The University of Hong Kong, Hong Kong, China*

(Received 1 September 2010; published 22 September 2010)

We have studied a quinary Fe-based superconductor $\text{Sr}_2\text{VFeAsO}_3$ by the measurements of x-ray diffraction, x-ray absorption, Mössbauer spectrum, resistivity, magnetization, and specific heat. This apparently undoped oxyarsenide is shown to be self-doped via electron transfer from the V^{3+} ions. We observed successive magnetic transitions within the VO_2 layers: an antiferromagnetic transition at 150 K followed by a weak ferromagnetic transition at 55 K. The spin orderings within the VO_2 planes are discussed based on mixed valence of V^{3+} and V^{4+} .

DOI: [10.1103/PhysRevB.82.104518](https://doi.org/10.1103/PhysRevB.82.104518)

PACS number(s): 74.70.Xa, 71.28.+d, 74.10.+v, 75.30.Kz

I. INTRODUCTION

The discovery of high-temperature superconductivity (HTSC) in layered Fe-based compounds^{1,2} represents an important breakthrough in the field of condensed-matter physics. So far, dozens of Fe-based superconductors in several crystallographic types have been discovered.² The common structural unit for the HTSC is Fe_2X_2 ($X=\text{As, Te, etc.}$) layers. The undoped Fe_2X_2 layers with formally divalent iron usually exhibit antiferromagnetic (AFM) spin-density-wave (SDW) instability.^{3,4} HTSC emerges as the SDW ordering is suppressed by various kinds of doping^{1,5–10} or applying pressures.¹¹ Both the magnetic ordering and superconductivity were suggested to be related to the nesting between the two cylinderlike Fermi surfaces near Γ and M points.^{12–16}

Recently, superconductivity at 37 K was reported in a quinary oxyarsenide $\text{Sr}_2\text{VFeAsO}_3$ (hereafter called V21113),¹⁷ consisting of perovskitelike $\text{Sr}_4\text{V}_2\text{O}_6$ and antiferrotype-type Fe_2As_2 block layers. The observed superconductivity *without extrinsic doping* challenges the above paradigm, and immediately aroused several first-principles calculations.^{18–22} However, the occurrence of superconductivity in the apparently undoped V21113 has not been clarified. Moreover, the calculated property of the $\text{Sr}_4\text{V}_2\text{O}_6$ layers is very much scattered: including magnetic half-metallic,¹⁸ nonmagnetic metallic,^{19,20} and magnetic (Mott-type) insulating²² states. Various kinds of possibilities on the magnetic ground state for V21113 were evaluated but no conclusive result was given.²¹ Experimentally, few works^{17,23} have been devoted to this system. It is simply not clear whether the Fe-site AFM order survives, let alone the magnetic property of the $\text{Sr}_4\text{V}_2\text{O}_6$ layers. The valence state of V, which is very crucial to understand the appearance of superconductivity, remains a puzzle. X-ray photoelectron spectroscopy (XPS) measurement suggested an “unexpected” V^{5+} even in the oxygen-deficient V21113 samples, however, the result was then questioned because of the surface-sensitive nature for the XPS method.²³

In this paper, we report systematic experimental studies on the structure and physical properties of V21113. We employed x-ray absorption spectroscopy, capable of detecting the bulk properties, to examine the valence state of V. Our data unambiguously reveal mixed valence of V^{3+} and V^{4+} , indicating that the Fe_2As_2 layers are actually self-doped due to the electron charge transfer from V to Fe. Our measurements have also identified two magnetic transitions at 55 K and 150 K, respectively, associated with the VO_2 layers. The observed weak ferromagnetism below 55 K and its coexistence with superconductivity at low temperatures make the V21113 system very unique in the family of Fe-based superconductors.

II. EXPERIMENTAL

Synthesis of single-phase 21113 samples turned out to be difficult¹⁷ because of the tendency of nonstoichiometry²⁴ as well as the multi-interphase solid-state reactions. We have improved the sample quality by carefully controlling the stoichiometry. Samples of $\text{Sr}_2\text{V}_{1-x}\text{Mg}_x\text{FeAsO}_3$ ($x=0$ corresponds to undoped V21113 and $x=0.1$ refers to Mg-doped sample) were prepared using fine powders (~ 200 mesh, purity $\geq 99.9\%$) of SrO, MgO, V, Fe, Fe_2O_3 , and As. The accurately weighed stoichiometric mixture was loaded in an alumina tube, preventing possible reactions with the quartz tube. The alumina tube, placed in a sealed quartz ampoule, was heated slowly to 1273 K, holding for 24 h. After the first time sintering, the sample was thoroughly ground, pressed into pellets, and sintered again in vacuum ($< 10^{-4}$ Pa) at 1353 K for 48 h. All the operations of weighing, mixing, grinding, pelletizing, etc., were carried out in an argon-filled glove box with the water and oxygen contents less than 0.1 ppm.

Several measurements were performed as follows. Powder x-ray diffraction (XRD) was carried out using a D/Max-rA diffractometer with $\text{Cu } K\alpha$ radiation and a graph-

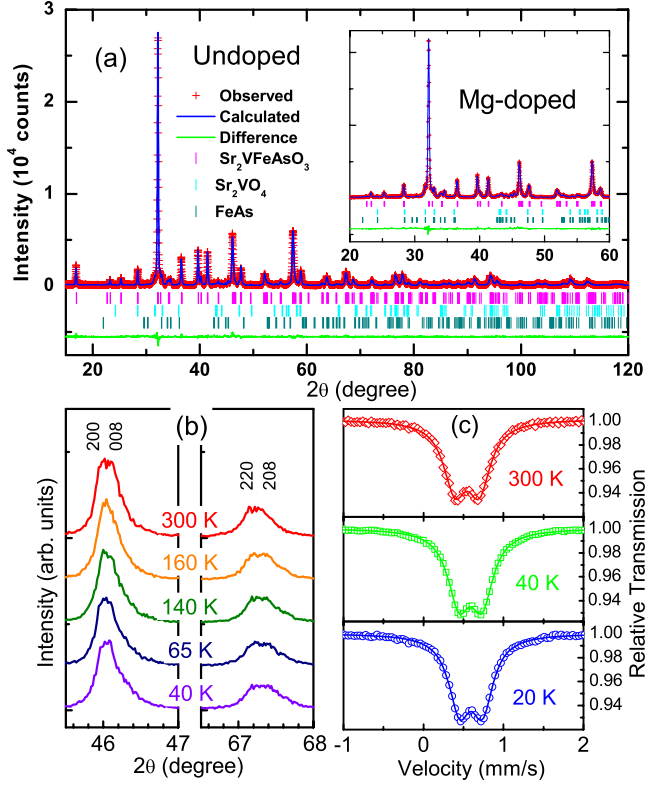


FIG. 1. (Color online) (a) Rietveld refinement profiles for the XRD data of $\text{Sr}_2\text{V}_{1-x}\text{Mg}_x\text{FeAsO}_3$ [$x=0$ and 0.1 (inset)]. (b) Selected XRD peaks at various temperatures. (c) ^{57}Fe Mössbauer spectra at different temperatures.

ite monochromator. The crystal structure at room temperature was refined by Rietveld analysis. The V K -edge x -ray absorption spectra (XAS) were measured in transmission mode using powdered samples on beam lines U7B and U7C at the National Synchrotron Radiation Facility (NSRF), Hefei, China. The water-cooled Si (111) plane bicrystal monochromator was used. Calibration of spectrometer was made using vanadium metal foil. The raw data were normalized according to the previous literature.²⁵ Mössbauer spectra were collected using a conventional constant acceleration drive. The sources were 50 mCi $^{57}\text{Co}:\text{Rh}$. The velocity calibration was performed with an α -iron foil at room temperature. The reported isomer shift (IS) values for iron are relative to the Fe foil. The resistivity was measured on bar-shaped samples using a standard four-terminal method. We employed Quantum Design PPMS-9 (physical property measurement system) and MPMS-5 (magnetic property measurement system) to measure the specific heat and dc magnetization, respectively.

III. RESULTS AND DISCUSSION

The XRD patterns are shown in Fig. 1(a). In comparison with the previous report,¹⁷ the intensity of impurity peaks (relative to that of the main peak) at $2\theta \sim 32^\circ$ is greatly reduced, indicating that the sample's quality is significantly improved. According to the multiphase Rietveld refinement,²⁶ the amount of impurity phases Sr_2VO_4 and

TABLE I. Crystallographic data of $\text{Sr}_2\text{V}_{1-x}\text{Mg}_x\text{FeAsO}_3$ ($x=0$ and 0.1) at room temperature. The space group is $P4/nmm$. The atomic coordinates are as follows: Sr1 (0.25, 0.25, z); Sr2 (0.25, 0.25, z); V (0.25, 0.25, z); Fe (0.25, 0.75, 0); As (0.25, 0.25, z); O1 (0.25, 0.25, z); and O2 (0.25, 0.75, z). BVS refers to bond valence sum (Ref. 30), reflecting the formal valence of an ion investigated.

Compounds	$x=0$	$x=0.1$
a (Å)	3.9352(1)	3.9334(2)
c (Å)	15.6823(5)	15.7488(7)
V (Å ³)	242.86(1)	243.66(2)
R_{wp}	8.59	8.82
S	1.68	1.70
z of Sr1	0.8090(1)	0.8091(1)
z of Sr2	0.5857(1)	0.5865(1)
z of V	0.3080(2)	0.3074(2)
z of As	0.0893(1)	0.0880(2)
z of O1	0.4248(4)	0.4257(5)
z of O2	0.2934(3)	0.2952(4)
BVS _V for V ^{III}	2.95	N.V.
BVS _V for V ^{IV}	3.29	N.V.
BVS _V for V ^V	3.46	N.V.
V-O2-V angle (deg)	166.7(2)	168.8(2)
As-Fe-As angle (deg)	109.1(1)	109.7(1)

FeAs are less than 5%. The refined structural parameters for $\text{Sr}_2\text{V}_{1-x}\text{Mg}_x\text{FeAsO}_3$ ($x=0$ and 0.1) are listed in Table I. The lattice constants of undoped V21113 are a little larger than the reported values.¹⁷ The Mg substitution leads to a lattice elongation. The As-Fe-As angle is very close to the ideal value for a regular tetrahedron. On the other hand, the V-O2-V angle obviously deviates from 180° .

The low-temperature XRD experiments indicate no evidence of structural phase transition in the whole temperatures measured. Some of the data are shown in Fig. 1(b). First, the (200) peak does not separate within the experimental limit, suggesting no usual tetragonal-to-orthorhombic transition. Second, unlike the case in $R\text{FeAsO}$ ($R=\text{La}, \text{Sm}, \text{Gd}, \text{and Tb}$),^{27,28} no obvious splitting for the (220) peak can be seen. Thus, the SDW-ordering-related structural phase transition²⁸ can be ruled out in V21113. While the lattice parameters were found to decrease with decreasing temperature, the precise temperature dependence is expected to be measured by a future XRD study with synchrotron radiations.

The Mössbauer spectra [Fig. 1(c)] show a quadrupole doublet at all the temperatures, in contrast with the sextet line for the AFM SDW ordered state.^{27,29} From the data we deduced no effective paramagnetic moment, therefore, the iron does not carry magnetic moment on its own. Accordingly no magnetic ordering at the Fe sublattice is expected. The IS value is similar to those observed for other ferroarsenide systems,²⁹ suggesting that the iron is basically divalent.

Figure 2 shows the V K -edge XAS for V21113 and its reference vanadium oxides. It has been well established that, in a number of V compounds, the position of the character-

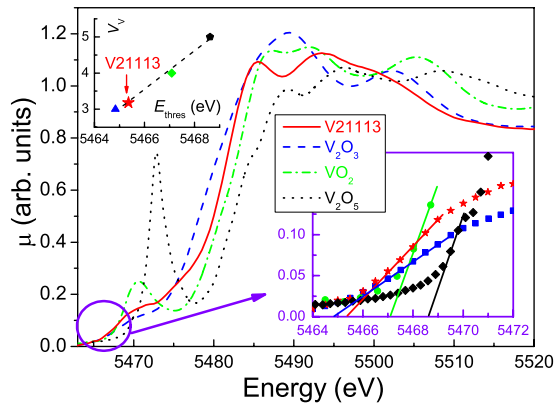


FIG. 2. (Color online) Vanadium K -edge x-ray absorption spectra for $\text{Sr}_2\text{VFeAsO}_3$ as well as some reference compounds V_2O_3 , VO_2 , and V_2O_5 . The insets show the determination of the valence of V (V_V) by the absorption threshold, E_{thres} .

istic absorptions (such as absorption threshold, pre-edge peak, and main absorption edge) varies linearly with the valence of V (V_V).²⁵ The main edge of V21113 lies in between those of V_2O_3 and VO_2 , clearly indicating the mixed valence state for V. The pre-edge structure (to the left of the main edge) of V21113 resembles that of V_2O_3 , suggesting that V^{3+} is dominant. One can fit the pre-edge of V21113 by the addition of weighed XAS of V_2O_3 and VO_2 . The best fitting gives $V_V=3.22$. In fact, V_V can be better determined by using the characteristic absorption threshold (E_{thres}). As shown in the insets of Fig. 2, E_{thres} increases steadily on going along $\text{V}_2\text{O}_3 \rightarrow \text{VO}_2 \rightarrow \text{V}_2\text{O}_5$. Assuming a linear relation of E_{thres} vs V_V , we obtain $V_V=3.18 \pm 0.05$, consistent with the former estimation. Here we note that the structural parameters of V21113 also support the conclusion about the V valence. The calculated bond-valence-sum³⁰ values for V in Table I verify the dominant V^{3+} with minority of V^{4+} in V21113.

Because of the overall charge neutrality, the mixed valence of V immediately suggests that the Fe_2As_2 layers are “self” (or internally) electron doped by the charge transfer from the V^{3+} ions (conversely, the $\text{Sr}_4\text{V}_2\text{O}_6$ layers are self-hole-doped). This conclusion is consistent with the measurements of Hall and Seebeck coefficients, which show electron-dominant transport behavior (not shown here), and also with the band calculations¹⁹ which indicate the occupation number of $3d$ electrons per V being less than 2. The absence of Fe-site AFM ordering and appearance of SC transition (see below) are thus naturally understood within the established paradigm for Fe-based HTSC.

In Fig. 3, we plot the temperature dependence of resistivity (ρ), magnetic susceptibility (χ), and specific heat (C) for V21113 along with $\text{Sr}_2\text{V}_{0.9}\text{Mg}_{0.1}\text{FeAsO}_3$ as a reference. The V21113 sample shows SC transition at 24 K, which is somewhat lower than previously reported.¹⁷ The lowered T_c is mainly ascribed to the “overdoped” state since the self-doping level achieves $\sim 18\%$ (from the obtained V_V above). As we see, the Mg-doped sample shows an enhanced T_c of 30 K. This result does suggest that the undoped V21113 be overdoped, because the Mg-for-V substitution induces holes, which partially compensates the heavy electron doping. Another reason for the lowered T_c could be due to the V-for-Fe

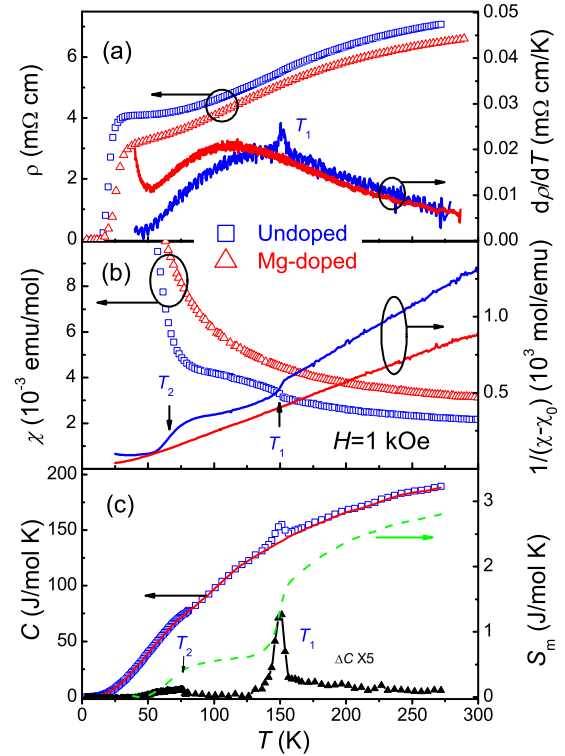


FIG. 3. (Color online) Temperature dependence of (a) resistivity, (b) magnetic susceptibility, and (c) specific heat for $\text{Sr}_2\text{VFeAsO}_3$ and $\text{Sr}_2\text{V}_{0.9}\text{Mg}_{0.1}\text{FeAsO}_3$. The left axes show the results after different data processing. χ_0 is 1.4×10^{-3} and 2.0×10^{-3} emu/mol for the undoped and Mg-doped samples, respectively.

antisite occupation, as suggested by a very recent report.³¹

For V21113, an anomaly at $T_1=150$ K is clearly shown in the derivative of $\rho(T)$ as well as $\chi(T)$ and $C(T)$ curves. In particular, the anomaly in $C(T)$ points to an intrinsic second-order phase transition since specific heat measures bulk properties (note that the amount of impurities is less than 5%). For the Mg-doped sample, however, such an anomaly is completely suppressed. Since the Fe-site magnetic ordering was ruled out by the above Mössbauer study, we conclude that the 150 K transition V21113 is intrinsic and directly related to the V atoms.

The $\chi(T)$ data in the range of $300 > T > 150$ K obey the Curie-Weiss law, $\chi = \chi_0 + C_{\text{Curie}} / (T - \theta_W)$, where C_{Curie} denotes the Curie constant and θ_W the Weiss temperature. Since the Fe atoms have no effective paramagnetic moments, as revealed by the above Mössbauer study, we can estimate the effective magnetic moments of V, which gives $P_{\text{eff}} = 1.2 \mu_B / V$ by the data fitting. The significantly lowered P_{eff} (compared with the spin-only value for either V^{3+} or V^{4+}) could be due to the d - p hybridization in connection with the mixed valence. The fitted θ_W value is 52 K, implying dominant ferromagnetic (FM) correlations between the magnetic moments. By subtracting $C(T)$ of Mg-doped V21113 from that of the undoped V21113, the magnetic entropy for the transition is calculated to be $\sim 1.1 \text{ J mol}^{-1} \text{ K}^{-1}$, which is much lower than the expected value of $R \ln(2S+1)$ ($S=1$ for V^{3+} and $S=1/2$ for V^{4+}). The result suggests that short-range magnetic order is established at the temperatures far above

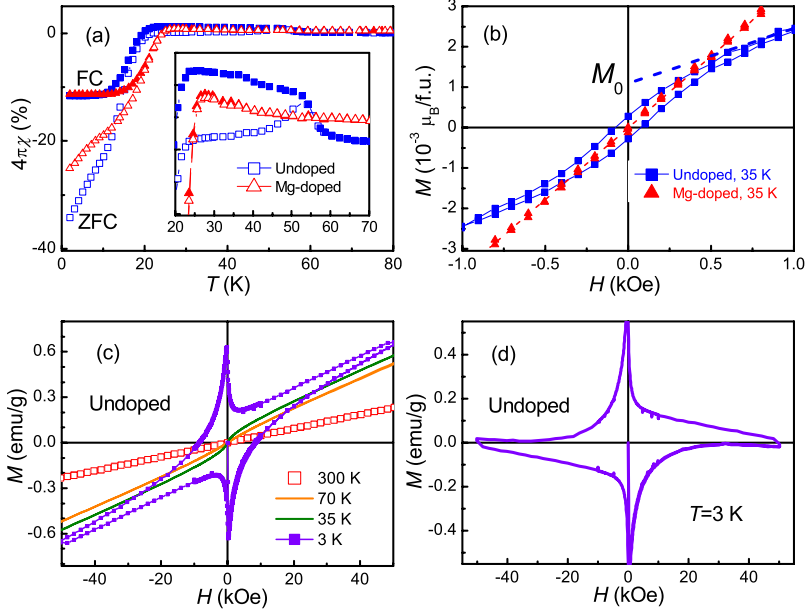


FIG. 4. (Color online) (a) Low-field $\chi(T)$ curves and (b) low-field $M(H)$ curves for $\text{Sr}_2\text{VFeAsO}_3$ (in comparison with the Mg-doped sample). Panel (c) shows a full-range $M(H)$ curves. Panel (d) displays the superconducting magnetization curve after subtracting a paramagnetic background.

150 K. Note that the steplike increase in χ at the transition does not mean a FM transition because the $M(H)$ curve for $70 < T < 150$ K is linear [see Fig. 4(c)]. In fact, the AFM ordering of A or C type possibly exhibits an increase in χ at the magnetic transition.³²

In addition to the 150 K transition, another anomaly at $T_2 \sim 55$ K can be clearly seen in $1/(\chi - \chi_0)$, as shown in Fig. 3(b). Specific-heat data also show a small anomaly around 55 K. However, the Mg-doped sample, which contains a little more impurities, *simultaneously* loses the two anomalies. This fact strongly suggests that the 55 K anomaly is also intrinsic and related to the $\text{Sr}_4\text{V}_2\text{O}_6$ layers. Figure 4 supplies more information about this second transition. At low fields, the magnetization diverges at 55 K for field-cooling (FC) and zero FC (ZFC) modes, suggesting a ferromagnetic transition. The FM state is further supported by the $M(H)$ curve, where a magnetic hysteresis loop is clearly observed. The very small extrapolated residual magnetization ($M_0 \sim 10^{-3} \mu_B/\text{V}$ at 35 K) and lack of saturation in M at high fields indicate that it is actually a weak FM (WFM). The WFM nature is consistent with the above Mössbauer spectra which show negligibly small transferred hyperfine field (below 0.07 T) at the Fe site for $T=20$ and 40 K. Nevertheless, the SC magnetic loop [Fig. 4(d)] exhibits obvious asymmetry relative to the horizontal axis, suggesting significant contributions of WFM in the SC state. It is noted that the coexistence of SC and WFM differs with the previous finding of the coexistence of SC and strong ferromagnetism (due to $4f$ local moments) in $\text{EuFe}_2(\text{As}_{0.7}\text{P}_{0.3})_2$.¹⁰

Now, let us discuss the possible origin of the two magnetic transitions within the $\text{Sr}_4\text{V}_2\text{O}_6$ layers. The electronic configurations of V^{3+} and V^{4+} are d^2 and d^1 , respectively. Within an ionic model, the lowest V $3d$ orbitals are degenerate d_{yz} and d_{xz} due to the crystal-field splitting. In the case of pure V^{3+} , the electron occupation is $d_{yz}^\uparrow d_{xz}^\uparrow$ according to the Hund's rule. The ground state of the square lattice of V in the VO_2 planes is AFM due to superexchange interaction.³² In $\text{V}_2\text{I}_{11}\text{3}$, there are $\sim 18\%$ V^{4+} ions and the Zener's double

exchange favors ferromagnetic spin arrangement in the same VO_2 plane for the gain of kinetic energy. This could result in an in-plane FM state. However, the electron hopping integrals in VO_2 planes are direction dependent. The amplitude of the hopping integral of d_{xz} along y axis (or d_{yz} along x axis), t' , is much smaller than that of d_{xz} along x axis (or d_{yz} along y axis), t . This leads to another possible spin array in the VO_2 planes, i.e., a C -type AFM state where the spins are parallel along x axis and antiparallel along y axis, or vice versa. By a simplified mean-field analysis, we estimate that the FM state is more stable if $|t'|/J > 2(1 - \delta)/\delta$, with J the neighboring spin coupling and δ the concentration of V^{4+} .

The scenario of in-plane FM state coincides with the aforementioned positive Weiss temperature. Thus the observed transition at $T_1 = 150$ K may be ascribed to an A -type AFM ordering with AFM coupling along the c axis. The WFM transition at $T_2 = 55$ K may be interpreted as the spin canting within the framework of double exchange proposed by de Gennes,³³ although usually one would expect a more substantial magnetic moment. As for the scenario of in-plane C -type AFM, the WFM transition is still an open question. One possibility is due to the nonzero Dzyaloshinsky-Moriya interaction, which plays an important role for the intriguing magnetic responses in other vanadium oxides.³⁴

IV. CONCLUDING REMARKS

To summarize, we have demonstrated experimentally that superconductivity in undoped $\text{Sr}_2\text{VFeAsO}_3$ is induced by a self-doping mechanism, i.e., an interlayer charge transfer from V to Fe. Neither structural phase transition nor Fe-site SDW ordering was observed, consistent with the electron-doped state in the Fe_2As_2 layers. In addition, we have identified two intrinsic magnetic transitions in connection with the mixed valence of V. The transition at 150 K is ascribed as an AFM ordering. The following transition at 55 K is weakly ferromagnetic, probably due to a spin canting process. The WFM transition renders a rare example of coexistence of SC

and WFM, which will be of great interest for the future studies. Further experiments such as neutron diffractions are desirable to check the spin structure of V and to confirm that the moment does not come from Fe.

ACKNOWLEDGMENTS

This work was supported by the NSF of China (Grant No. 90922002), National Basic Research Program of China

(Grant No. 2007CB925001), and the Fundamental Research Funds for the Central Universities of China (Grant No. 2010QNA3026). The research in Jerusalem is supported by the Israel Science Foundation (Bikura Grant No. 459/09) and by the joint German-Israeli DIP project. F.C.Z. acknowledges partial support from Hong Kong RGC under Grant No. HKU 7068/09P and NSF/RGC under Grant No. N-HKU 726/09. The authors would like to thank NSRL for the synchrotron radiation beam time.

*Corresponding author; ghcao@zju.edu.cn

- ¹Y. Kamihara, T. Watanabe, M. Hirano, and H. Hosono, *J. Am. Chem. Soc.* **130**, 3296 (2008).
- ²For a recent review, see D. Johnston, [arXiv:1005.4392](https://arxiv.org/abs/1005.4392), Adv. Phys. (to be published).
- ³C. de la Cruz, Q. Huang, J. W. Lynn, J. Li, W. Ratcliff II, J. L. Zarestky, H. A. Mook, G. F. Chen, J. L. Luo, N. L. Wang, and P. Dai, *Nature (London)* **453**, 899 (2008).
- ⁴Q. Huang, Y. Qiu, W. Bao, M. A. Green, J. W. Lynn, Y. C. Gasparovic, T. Wu, G. Wu, and X. H. Chen, *Phys. Rev. Lett.* **101**, 257003 (2008).
- ⁵Z. A. Ren, J. Yang, W. Lu, W. Yi, X. L. Shen, Z. C. Li, G. C. Che, X. L. Dong, L. L. Sun, F. Zhou, and Z. X. Zhao, *EPL* **82**, 57002 (2008).
- ⁶H. H. Wen, G. Mu, L. Fang, H. Yang, and X. Zhu, *EPL* **82**, 17009 (2008).
- ⁷C. Wang, L. Li, S. Chi, Z. Zhu, Z. Ren, Y. Li, Y. Wang, X. Lin, Y. Luo, S. Jiang, X. Xu, G. Cao, and Z. Xu, *EPL* **83**, 67006 (2008).
- ⁸A. S. Sefat, A. Huq, M. A. McGuire, R. Y. Jin, B. C. Sales, D. Mandrus, L. M. D. Cranswick, P. W. Stephens, and K. H. Stone, *Phys. Rev. B* **78**, 104505 (2008); C. Wang, Y. K. Li, Z. W. Zhu, S. Jiang, X. Lin, Y. K. Luo, S. Chi, L. J. Li, Z. Ren, M. He, H. Chen, Y. T. Wang, Q. Tao, G. H. Cao, and Z. A. Xu, *ibid.* **79**, 054521 (2009).
- ⁹G. H. Cao, S. Jiang, X. Lin, C. Wang, Y. K. Li, Z. Ren, Q. Tao, C. M. Feng, J. H. Dai, Z. A. Xu, and F. C. Zhang, *Phys. Rev. B* **79**, 174505 (2009).
- ¹⁰Z. Ren, Q. Tao, S. Jiang, C. M. Feng, C. Wang, J. H. Dai, G. H. Cao, and Z. A. Xu, *Phys. Rev. Lett.* **102**, 137002 (2009).
- ¹¹M. S. Torikachvili, S. L. Budko, N. Ni, and P. C. Canfield, *Phys. Rev. Lett.* **101**, 057006 (2008).
- ¹²D. J. Singh and M.-H. Du, *Phys. Rev. Lett.* **100**, 237003 (2008).
- ¹³J. Dong, H. J. Zhang, G. Xu, Z. Li, G. Li, W. Z. Hu, D. Wu, G. F. Chen, X. Dai, J. L. Luo, Z. Fang, and N. L. Wang, *EPL* **83**, 27006 (2008).
- ¹⁴I. I. Mazin, D. J. Singh, M. D. Johannes, and M. H. Du, *Phys. Rev. Lett.* **101**, 057003 (2008).
- ¹⁵K. Kuroki, S. Onari, R. Arita, H. Usui, Y. Tanaka, H. Kontani, and H. Aoki, *Phys. Rev. Lett.* **101**, 087004 (2008).
- ¹⁶K. Terashima, Y. Sekiba, J. H. Bowen, K. Nakayama, T. Kawahara, T. Sato, P. Richard, Y. M. Xu, L. J. Li, G. H. Cao, Z. A. Xu, H. Ding, and T. Takahashi, *Proc. Natl. Acad. Sci. U.S.A.* **106**, 7330 (2009).
- ¹⁷X. Y. Zhu, F. Han, G. Mu, P. Cheng, B. Shen, B. Zeng, and H. H. Wen, *Phys. Rev. B* **79**, 220512(R) (2009).
- ¹⁸I. R. Shein and A. L. Ivanovskii, *J. Supercond. Novel Magn.* **22**, 613 (2009).
- ¹⁹K. W. Lee and W. E. Pickett, *EPL* **89**, 57008 (2010).
- ²⁰G. Wang, M. Zhang, L. Zheng, and Z. Yang, *Phys. Rev. B* **80**, 184501 (2009).
- ²¹I. I. Mazin, *Phys. Rev. B* **81**, 020507(R) (2010).
- ²²H. Nakamura and M. Machida, *Phys. Rev. B* **82**, 094503 (2010).
- ²³F. Han, X. Y. Zhu, G. Mu, P. Cheng, B. Shen, B. Zeng, and H. H. Wen, *Sci. China, Ser. G* **53**, 1202 (2010).
- ²⁴M. Tegel, F. Hummel, Y. X. Su, T. Chatterji, M. Brunelli, and D. Jorhendt, *EPL* **89**, 37006 (2010).
- ²⁵J. Wong, F. W. Lytle, R. P. Messmer, and D. H. Maylotte, *Phys. Rev. B* **30**, 5596 (1984).
- ²⁶The reliable factors of the refinement are $R_{wp}=0.086$ and $R_{exp}=0.051$, indicating a fairly good accuracy for the structural parameters obtained.
- ²⁷M. A. McGuire, A. D. Christianson, A. S. Sefat, B. C. Sales, M. D. Lumsden, R. Y. Jin, E. A. Payzant, D. Mandrus, Y. B. Luan, V. Keppens, V. Varadarajan, J. W. Brill, R. P. Hermann, M. T. Sougrati, F. Grandjean, and G. J. Long, *Phys. Rev. B* **78**, 094517 (2008).
- ²⁸Y. K. Luo, Q. Tao, Y. K. Li, X. Lin, L. J. Li, G. H. Cao, Z. A. Xu, Y. Xue, H. Kaneko, A. V. Savinkov, H. Suzuki, C. Fang, and J. P. Hu, *Phys. Rev. B* **80**, 224511 (2009).
- ²⁹I. Nowik and I. Felner, *Physica C* **469**, 485 (2009).
- ³⁰I. D. Brown and D. Altermatt, *Acta Crystallogr., Sect. B: Struct. Sci.* **41**, 244 (1985).
- ³¹M. Tegel, T. Schmid, T. Stürzer, M. Egawa, Y. Su, A. Senyshyn, and D. Jorhendt, [arXiv:1008.2687](https://arxiv.org/abs/1008.2687) (unpublished).
- ³²J. S. Zhou, J. B. Goodenough, J. Q. Yan, and Y. Ren, *Phys. Rev. Lett.* **99**, 156401 (2007).
- ³³P.-G. de Gennes, *Phys. Rev.* **118**, 141 (1960).
- ³⁴Y. Ren, T. T. M. Palstra, D. I. Khomskii, E. Pellegrin, A. A. Nugroho, A. A. Menovsky, and G. A. Sawatzky, *Nature (London)* **396**, 441 (1998).